NEW ZEALAND SOCIETY FOR EARTHQUAKE ENGINEERING
2019 Pacific Conference on Earthquake Engineering
TURNING HAZARD AWARENESS INTO RISK MITIGATION
4 – 6 April | SkyCity, Auckland | New Zealand

AEES Reconnaissance Mission to Papua New Guinea, March/April 2018

Cvetan Sinadinovski
Global SeismiCS, Canberra ACT, Australia.

Kevin F. McCue
Central Queensland University, Rockhampton University, Qld, Australia.

Gary Gibson
Seismology Research Centre, Victoria, Australia.

Agus Abdulah
Geophysical Engineering Dept., Pertamina Uni., Indonesia.

David Love
Australian Seismological Association, Adelaide, SA, Australia.

ABSTRACT

A major magnitude 7.5 earthquake struck the Central Highlands of Papua New Guinea (PNG) on 26 February 2018 causing 160 deaths, hundreds of injuries and widespread destructive landslides. Operations of the major petroleum and mining industry in PNG were shut down. An energetic sequence of aftershocks followed including 6 of magnitude 6 or more.

The nearest available seismographs were more than 500km away resulting in large uncertainties in focal depth and poor location of most of the aftershocks. With substantial assistance from Oil Search Ltd., two seismologists representing the Australian Earthquake Engineering Society (AEES) installed 6 accelerographs in the epicentral region 3 weeks after the mainshock to monitor aftershocks.

Strong shaking was recorded at 200 samples/second continuously on all 6 accelerographs during the last of the magnitude 6 aftershocks on 7 April 2018. The horizontal pga was in excess of 0.67g at a distance of 35km and strong shaking lasted more than 10 seconds. Several thousand smaller

aftershocks were recorded and some 200 of them have been located. Aftershock foci occurred over a depth range of near surface to about 40km, all within the crust.

Geotomography software was used to invert near-field P and S travel times from more than 100 aftershocks to constrain velocity/depth relationships in the fault zone. Three dimensional corrections to the adopted crustal model were obtained including a velocity perturbation under the large intraplate volcano, Mt Bosavi.

These new results will allow better understanding of the seismicity and tectonics in the Southern Highlands of Papua New Guinea and contribute in improvement of its hazard maps and the next earthquake code.

1 INTRODUCTION

This study is based on the work done by a group of Australian seismologists in the aftermath of the major magnitude 7.5 earthquake on the southern side of the Central Highlands of Papua New Guinea, on 26 February at 17:44 UTC. More than 160 people were reported killed and many other injured in several provinces (McCue at al., 2018). An aftershock of magnitude 6.0 killed 11 people on 4 March at 19:56 UTC, while another aftershock of magnitude 6.7 on 6 March at 14:13 UTC killed at least 25 more. A magnitude 6.3 aftershock killed another 4 people on April 7 at 05:48 UTC, more than a month after the first tremors hit the area.

The Australian Earthquake Engineering Society in conjunction with the Oil Search funded seismologists Kevin McCue and Gary Gibson on a field trip to PNG. They deployed six accelerographs starting the 19th March to monitor aftershocks (McCue et al., 2018; Gibson et al., 2018). The instruments recorded thousands of aftershocks including one on 7th April with magnitude M6.3. The accelerograms obtained were tomographically inverted to constrain the velocity/depth relationships under the fault zone of the February 2018 major event (Sinadinovski et al., 2018).

2 SEISMOTECTONICS

The earthquake source was movement on a shallow fault or series of faults that failed under the unrelenting collision of the Australian and Pacific Plates. A number of large shear-gouge fragments, sub-plates or continental fragments, separate the two plates in the Papua New Guinea region in this complex mega shear zone that has resulted from their collision over several millions of years.

A continuous relatively narrow band of earthquake along the Southern Highlands marks the northern edge of the Australian Plate and this series of crustal earthquakes occurred along that boundary. Their focal mechanisms are predominantly shallow thrusts striking WNW, parallel to the uplifted mountains (Ripper and McCue, 1983).

The regional geology and borehole measurements show a complex crustal structure in the plate boundary environment, where an unknown thickness of deformed Australian Plate crust is overlain by a 3km thick sedimentary sequence.

St John (1967) used gravity data to model the Moho thickness under New Guinea as shown in Figure 1.

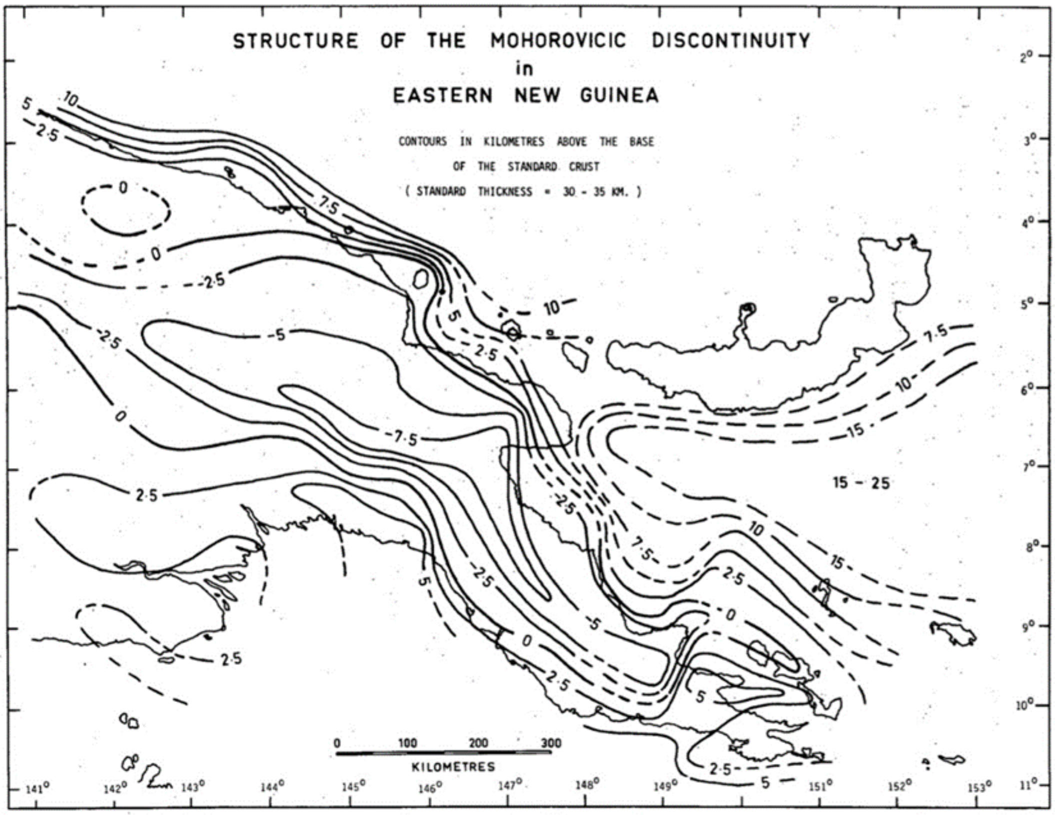

Figure 1: Structure of the Moho discontinuity in the Eastern New Guinea according to St. John, 1967

Since isoline 0 is set to 30-35km, than the isolines of -7.5 over the Southern Highlands of PNG will mean expected Moho at 37.5-42.5km.Those values can be compared with the measurements on the Australian side.

The Australian continent is relatively well covered with both active and passive seismic techniques. Multiple sources of information are therefore available for building a model of Moho depth (Salmon et al., 2012). Results from on-shore and off-shore refraction experiments are supplemented by receiver functions from a large number of portable stations and the recently augmented set of permanent stations. The composite data set provides good sampling of much of Australia, though coverage remains low in some remote desert areas. The various datasets provide multiple estimates of the depth to Moho in many regions, and the consistency between the different techniques is high.

Although at the edge of the Australian Moho map constructed from the full set of available seismological estimates, the results are in general agreement for the areas underneath the Southern Highlands of PNG, where its depth from the surface is approximately 40km.

3 SEISMICITY

Seismicity in the PNG region is characterised with frequent large earthquakes. Since 1900 there have been 22 earthquakes with magnitude M≥7.5. The dominant earthquake mechanisms are thrust and strike slip, associated with the arc-continent collision and the relative motions between numerous smaller plates. The largest earthquake in the region was a magnitude M8.2 shallow thrust fault event in the northern Papua province of Indonesia that killed 166 people in 1996 (Seismicity of the Earth 1900–2010, New Guinea and vicinity: U.S. Geological Survey Open-File Report 2010–1083-H).

At 3:44am on the morning of 26 February 2018 (17:44 UTC on 25 February) a very strong earthquake shook the Southern Highlands of Papua New Guinea. McCue et. al. 2018, describe that the occupants in oil/gas company camps between Moro and Komo reported shock and fear as their beds shot backwards and forwards across the room, cupboards rocked and toppled over.

The average duration of strong shaking in the Moro region was reported as about a minute. The situation for the local villagers was more than 160 deaths, many more injuries and people missing. Several lightly reinforced buildings collapsed in Tari and Mendi due to the strong shaking causing loss of life and casualties, but the hospital at Tari, an old single-story timber framed building on a concrete slab seems to have suffered little damage. At least 26,000 people were displaced, and 275,000 people were in urgent need of emergency supplies. The quake and its aftershocks caused panic and some damage in West Papua and, unusually, shaking was noticeable in northern Queensland and the Torres Strait islands.

An interesting helicopter view at 142.9844°E, 6.3396°S, 28km west of Moro, shows a fault blocked Tagari River (Fig. 2) which has finally cut through and started draining the impounded water and mud..

Figure 2: Air photo of blocked Tagari River, looking southward, the arrows marking the fault

A satellite view in Figure 3 shows the same section of river at a smaller scale, the short fault segment, river blockage and offset quite clear. The strongly faulted terrain can be inferred.

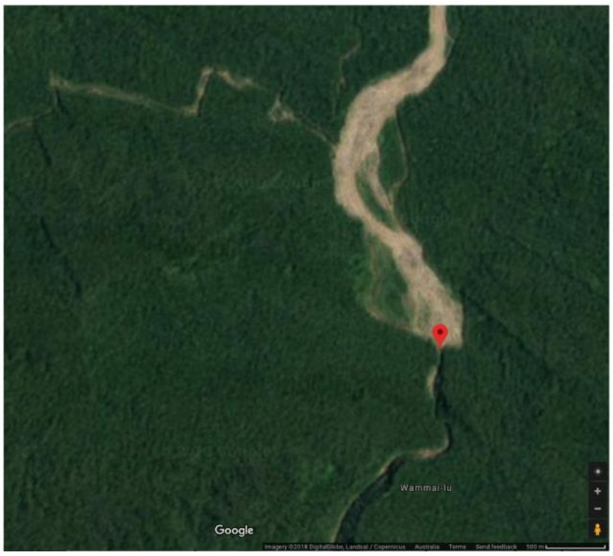

Figure 3: Satellite image from Google Earth showing the 1km long fault offset along the Tagari River photographed from the helicopter in the previous figure

The earthquake source was movement on a fault or, more probably, series of faults that failed under the unrelenting collision of the Australian and Pacific Plates, the former moving at about 7m per hundred years towards the NNE, the latter moving at 10m per hundred years towards the NW in the PNG region. A number of large shear-gouge fragments, sub-plates or continental fragments, separate the two plates in the Papua New Guinea region in this complex mega shear zone that has resulted from their collision over many millions of years (McCue et al., 2018).

A seismicity map of that area after the mainshock but prior to the installation of the network of six temporary stations is shown on Figure 4. The earthquake epicentres are represented by circles with radius proportional to their magnitude and the seismic stations are represented by black triangles, drawn over elevation contours. The temporary stations were deployed in such a pattern that they encircled the aftershock area in the best possible way for seismic data acquisition and further analysis (McCue et al., 2018; Gibson et al., 2018).

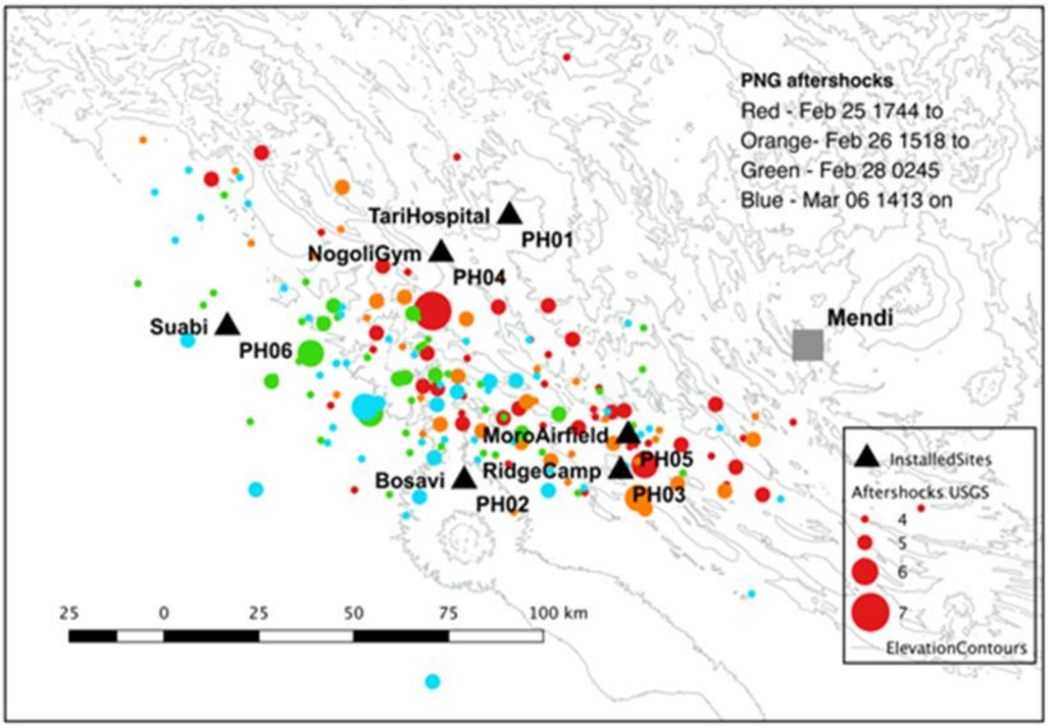

Figure 4: Seismicity map of the area prior to the installation period of the network of 6 temporary stations, drawn over a topographic map

Six Gecko recorders and SRC triaxial accelerographs were installed at Moro Airfield, Tari hospital, Nogoli, Mount Bosavi, Suabi and Ridge Camp sites. They are sensitive instruments powered by 12V batteries, with a GPS receiver so they have precisely the same timebase.

4 SEISMOGRAMS

The acquired data consisted of 3-component strong motion records recovered from the network for the M6.3 aftershock and hundreds of smaller events. The dataset from the largest aftershock recorded on 7th of April 2018 is also available through the aees.org.au website. Plotting of the waveforms (e.g. Fig. 5) and picking of the arrivals was done using a freeware package called Waves courtesy of Seismology Research Centre-SRC in Melbourne.

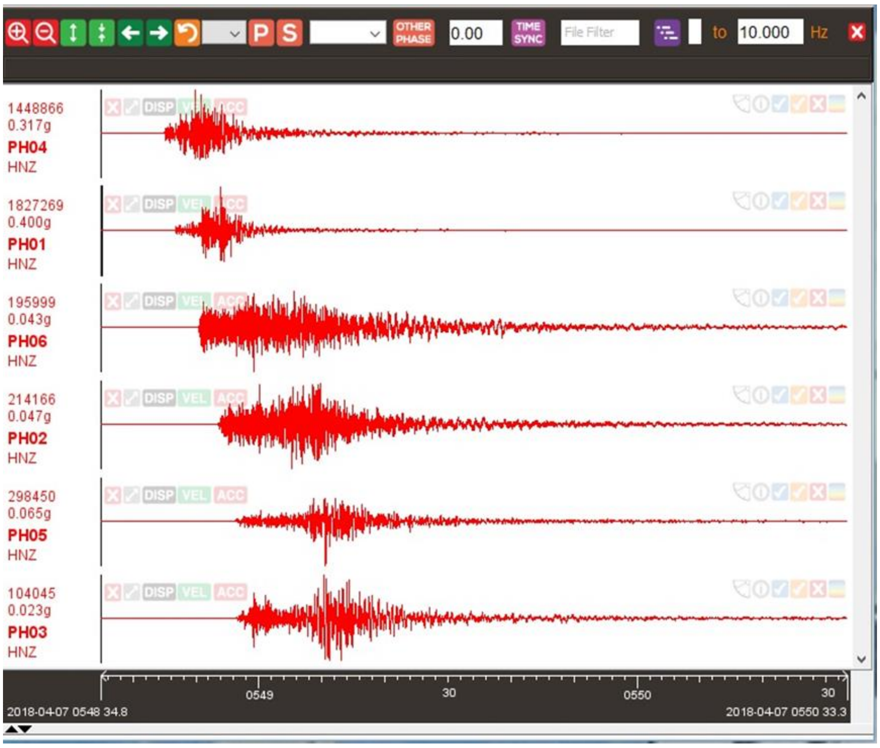

Figure 5: Seismograms (Vertical component) of the magnitude M6.3 aftershock at all the stations

Figure 6 shows the 3-Component seismic record of that aftershock on the nearest station Tari, at approximate distance of 35km from the focus. The horizontal Peak Ground Acceleration exceeded 0.63g, while the vertical registered 0.4g. The strongest shaking, with a duration of a 12 seconds, is in the surface waves coda that follow the P= and S-wave arrivals marked by the vertical thin black lines. The difference in the frequency content of the vertical and horizontal components is noticeable; the long period horizontal ground motion is probably from the Love waves generated in the near-surface crustal layers, while they are almost absent on the vertical component.

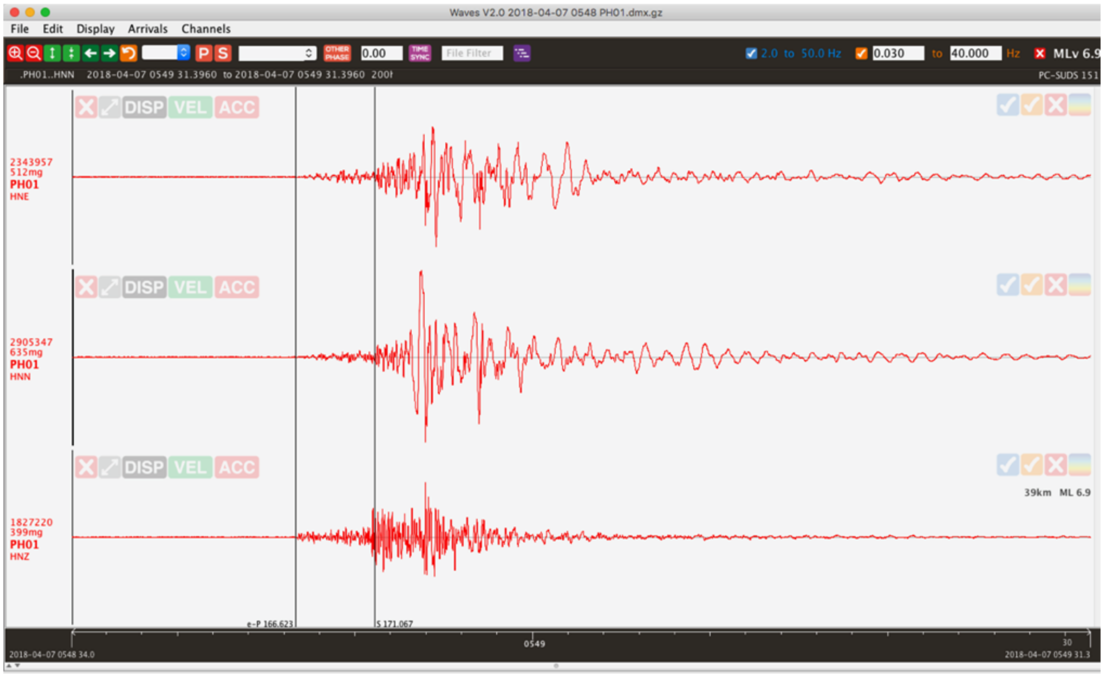

Figure 6: 3-C Seismogram of the magnitude M6.3 aftershock recorded at Tari station

5 DATA PROCESSING

To explore the crust under the Southern Highlands of PNG, the events that occurred in a cube of 2x2 degrees centred on the temporary network and down to 60km deep were processed. To investigate the 3-D structure underneath the area, the initial velocity model (McCue et al., 2018) was utilised as shown on Figure 7. The aim was to use the data to image the layers in the top and evaluate the Moho discontinuity.

The volume was discretised into cells of 15x15km grid in the surface area and depth ranges in the intervals of 3, 8, 15, 20, 28, 35, and 45 to 60km. After reviewing the seismograms, over 100 events were selected due to their origin distribution in depth and azimuth in respect to the location of the network. Thus, between 500 and 600 P-arrival times and corresponding number of S-arrival times were used in the tomographic analysis.

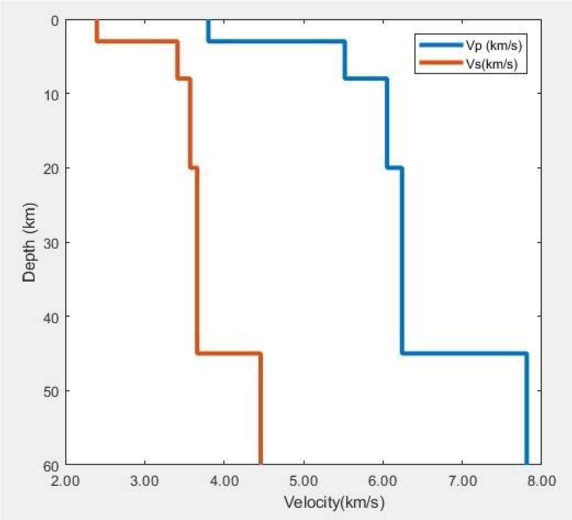

Figure 7: Initial velocity model utilised for the Southern Highlands of PNG

The ray paths and the coverage for the events and the recording stations over the topography of the study area are schematically presented in Figure 8. The cube has relatively good angular coverage in the area of interest and down to 45km, as there are only a few events deeper.

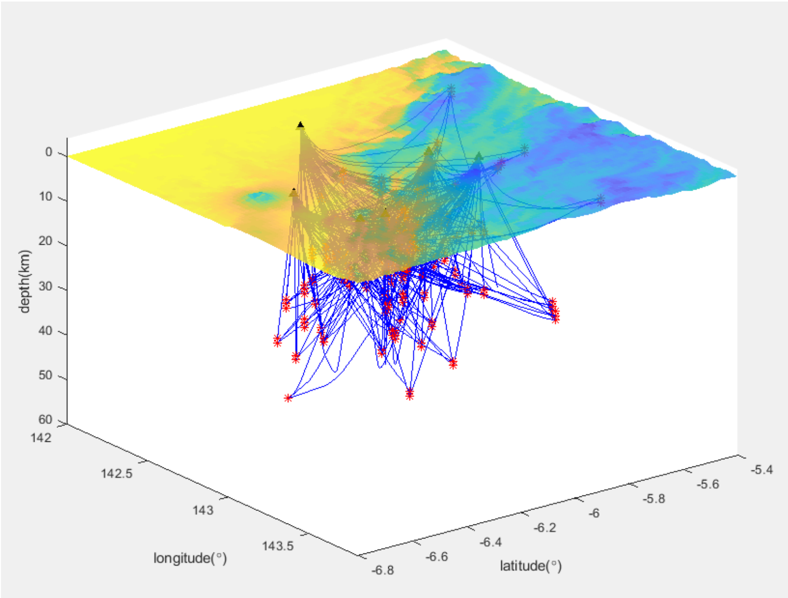

Figure 8: The ray paths and the coverage for the events and the receivers over the topography of the study area (earthquakes-red stars, stations-black triangles, ray paths-blue lines)

6 GEOTOMOGRAPHY

Fast Marching Method was applied in the tomographic inversion to simulate the arrival times for the source-receiver combinations (Sinadinovski et al, 2018). In that travel-time inversion, the observed P- and S-arrivals are compared with the calculated arrivals based on the initial model (from Fig.7) and the differences distributed over the ray paths. Each voxel that is criss-crossed by the ray paths gets a portion of that difference proportional to its part of the total ray length. In the iterative process, the difference between the observed and the calculated times is minimised and when it reaches values smaller than the reading error it stops.

In order to define the volume within the cube where we can have a confidence in the results, we performed a series of checkerboard tests for sensitivity of the tomographic inversion. It was found that with the given source-receiver combinations it is possible to recover the top half of the initial model after a small number of iterations, usually around five (Sinadinovski et al., 2018).

The tomography results are stored as a matrix of slowness perturbations in respect to the initial 3-D velocity model. The velocity matrix values can also be graphically shown at various slices through the cube, mostly horizontally and vertically. The novelty of this software package is its ability to be applied both in forward modelling and inversion, thus allowing the user to monitor in 3-D the effects of the re-location of the seismic events on the model composition.

The tomography results are displayed as slowness perturbations in respect to the initial velocity model given on Figure 7 at various slices through the cube. The colour bar represents blue-fast and red-slow values, while the recovered images can be viewed with confidence only in the cells crossed by the seismic rays, as indicated by the checkerboard tests.

Figure 9 shows the relative P-wave slowness perturbation in respect to the initial velocity model at various depths. It can be noticed a zone of fast velocity in the top layers oriented NW-SE, which is consistent with the general direction of the PNG highlands. Figure 10 shows the relative S-wave slowness perturbation in respect to the initial velocity model at the same depths. Similar trend can be noticed that a zone of fast velocity in the top layers is oriented NW-SE, which is consistent with the general direction of the PNG highlands. On both the north and south side of that zone, there are shallow discontinuous blocks with slower velocity of up to 1km/s.

Figure 11 shows the tomographic results for the checkerboard tests and longitudinal slices of relative slowness perturbation in respect to the initial velocity model; The N-S slices through the cube are taken from west to east, and on the colour bar the blue end represents fast, while the red end of the spectrum represents slow velocities. Once again, the images produced using the P- and S-arrivals look very similar, because the number of readings used in the inversion was very close.in both cases. The results in the second and the third vertical slice of the cube can be viewed with higher confidence. A slow velocity zone is noticeable on the images which is consistent with the actual position of the known volcano in the area.

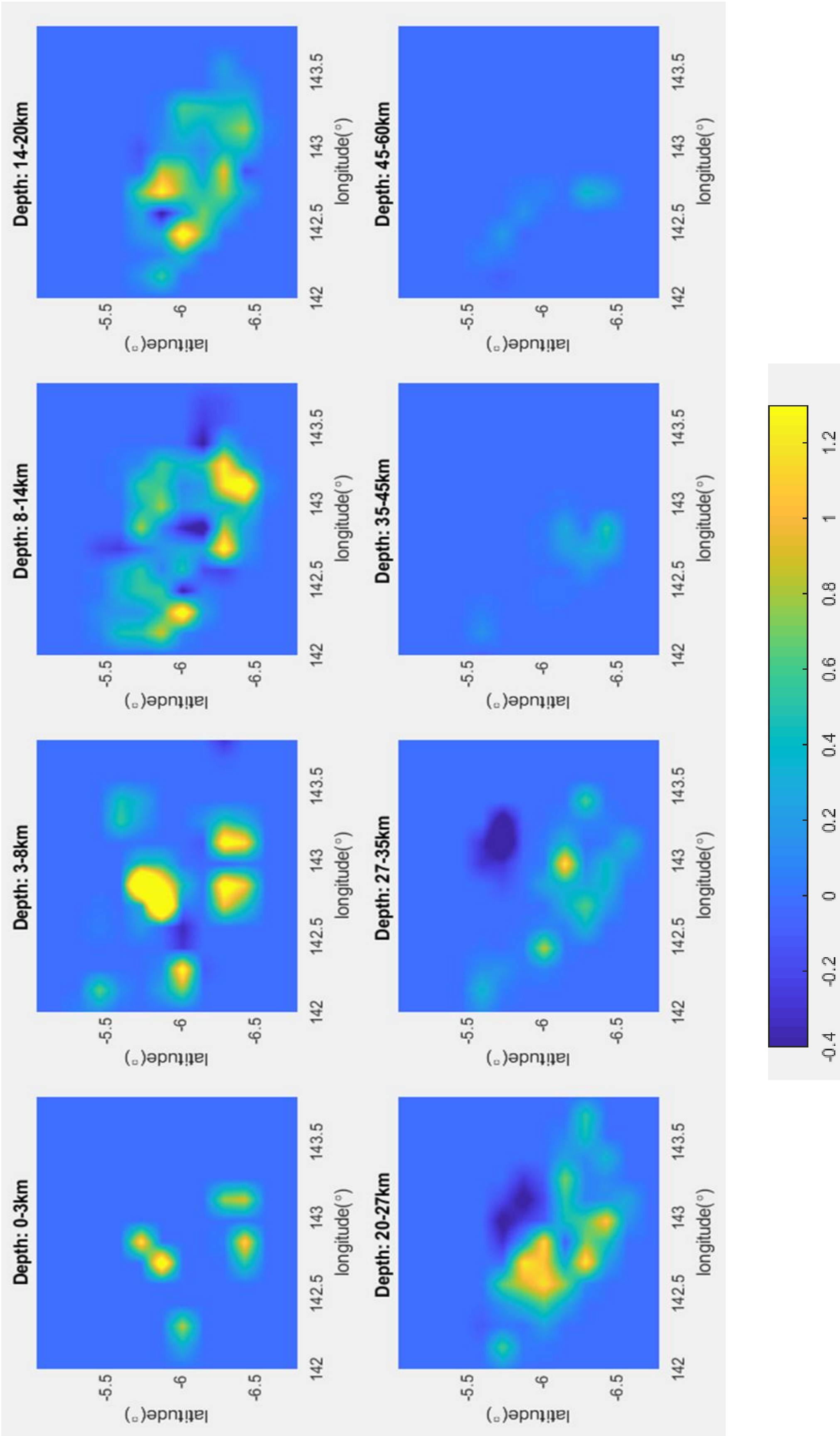

Figure 9: Relative P-wave slowness perturbation in respect to the initial velocity model at various depths; (Blue-fast, Red-Slow)

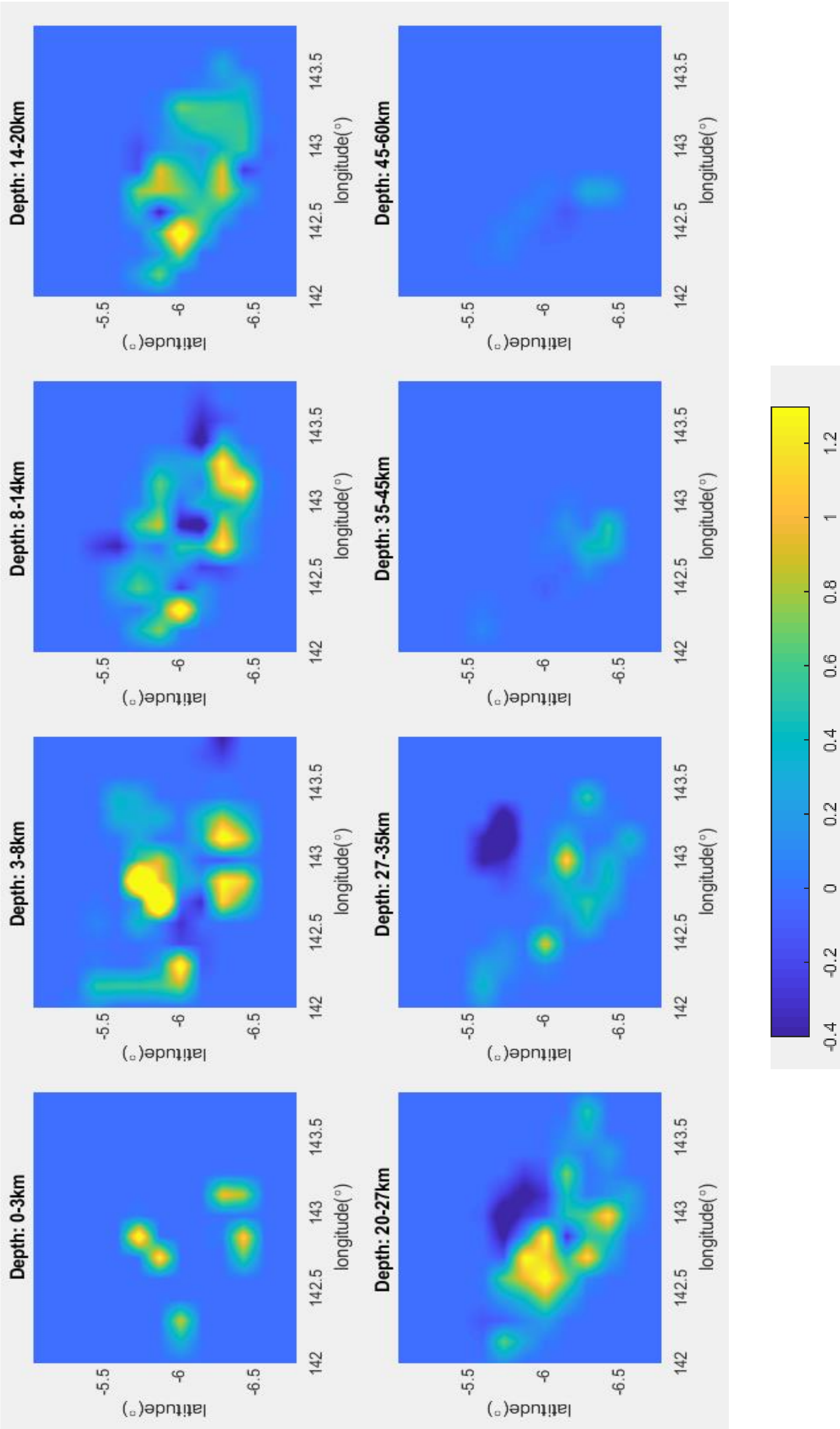

Figure 10: Relative S-wave slowness perturbation in respect to the initial velocity model at various depths; (Blue-fast, Red-Slow)

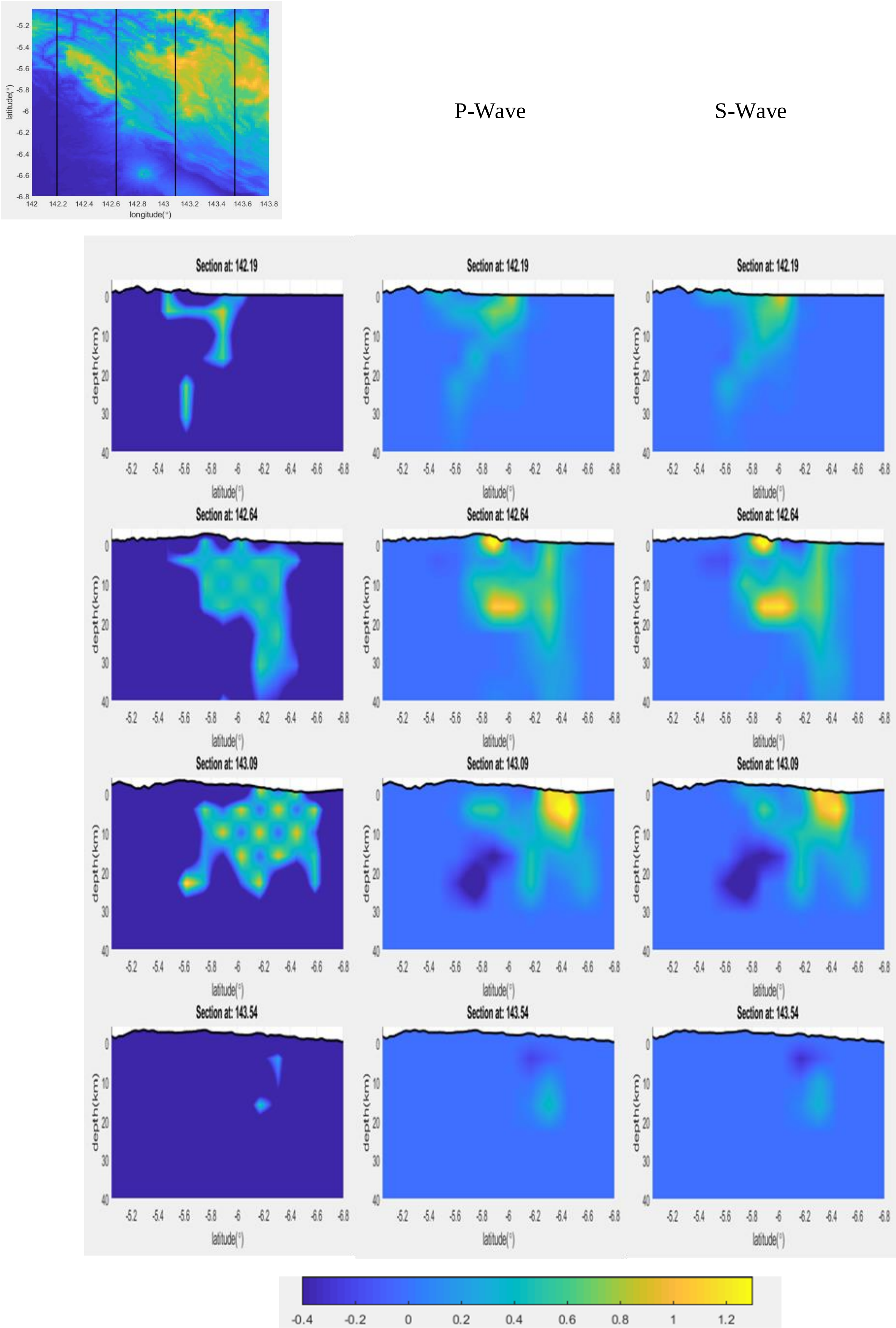

Figure 11: Checkerboard tests and longitudinal slices of relative slowness perturbation in respect to the initial velocity model; (Blue-fast, Red-Slow)

Figure 12 shows the tomographic results for the checkerboard tests and accompanied latitudinal slices of relative slowness perturbation in respect to the initial velocity model; The W-E slices through the cube are taken from north to south, and on the colour bar the blue end represents fast, while the red end of the spectrum represents slow velocities. The most northerly slice in the cube practically has no data to change the background velocity. The images produced using the P- and S-arrivals look very similar, due to the fact that the number of readings used in the inversion was very close.in both cases. The results in the second and the third vertical slice of the cube can be viewed again with higher confidence. A slow velocity zone coinciding with the known volcano Mt. Bosavi is noticeable on the southern side, with its imprint extending down to 20km. However, since that part of the area is not well covered by the rays, the deeper section may be the artefact of the tomography.

Three central SW-NE cross-sections of relative slowness perturbation in respect to the initial velocity model are shown on Figure 13. The vertical slices through the cube are taken as labelled from A to C, and on the colour bar the blue end of the spectrum represents fast, while the red end represents slow velocities. The slices are purposely chosen orthogonally to the orientation of the PNG highlands, to maximise the possibility of viewing the geological sections in comparison with the existing maps. The V-shape slow velocity zone on the images with a fast velocity in its middle can resemble situation of the compression from the north and south side, with a gently folded belt in between.

Three central NW-SE cross-sections of relative slowness perturbation in respect to the initial velocity model are shown on Figure 14. The vertical slices through the cube are taken as labelled from A to C, and on the colour bar the blue end of the spectrum represents fast, while the red end represents slow velocities. The slices are purposely chosen paralel to the orientation of the PNG highlands, to maximise the possibility of viewing the geological sections in comparison with the existing maps. The shape of the velocity zones on the images is consistent with the existing geological maps for the Papuan Belt area.

Other interpretations are also possible, depending on the cross-sections through the model cube. It has to be emphasised that more intermediate slices are possible, but the tomography results are comparatively stable and reflect the limitation of the source-receiver geometry and discretisation of the model cube.

6.1 Ground Motion Spectra

The software package Waves from SRC integrates the acceleration data into velocity and displacement waveforms, the velocity particularly useful for phase picking. It also plots Fourier spectra that are useful for picking the corner frequencies. In the case displayed in Figure 15 of the N29E component at Tari (PH01) the spectral amplitude is flat between 0.5s and 1.5s and drops off with higher frequency to the right and longer periods to the left. The flattening at long periods is probably due to strong surface waves. The drop off at high frequency can be measured for comparison with the generally assumed value of -2

7 DISCUSSION

This study is based on the work done in the aftermath of the major magnitude 7.5 earthquake in February 2018. Here, we compile the existing findings so far with an update of the results.

We have used a proxy crustal model to locate aftershocks that occurred under the Central Highlands of PNG over a month from 19 March. No pattern in the aftershocks that might indicate a distinct fault system can be discerned, rather the whole region is being sheared, thickened and uplifted by crustal shortening as reflected in the geology. One of the few cases of active surface faulting was observed during an overflight by helicopter, on ground verification was impossible but a careful study of aerial photography using drones is bound to throw-up other cases that may be accessible on the ground.

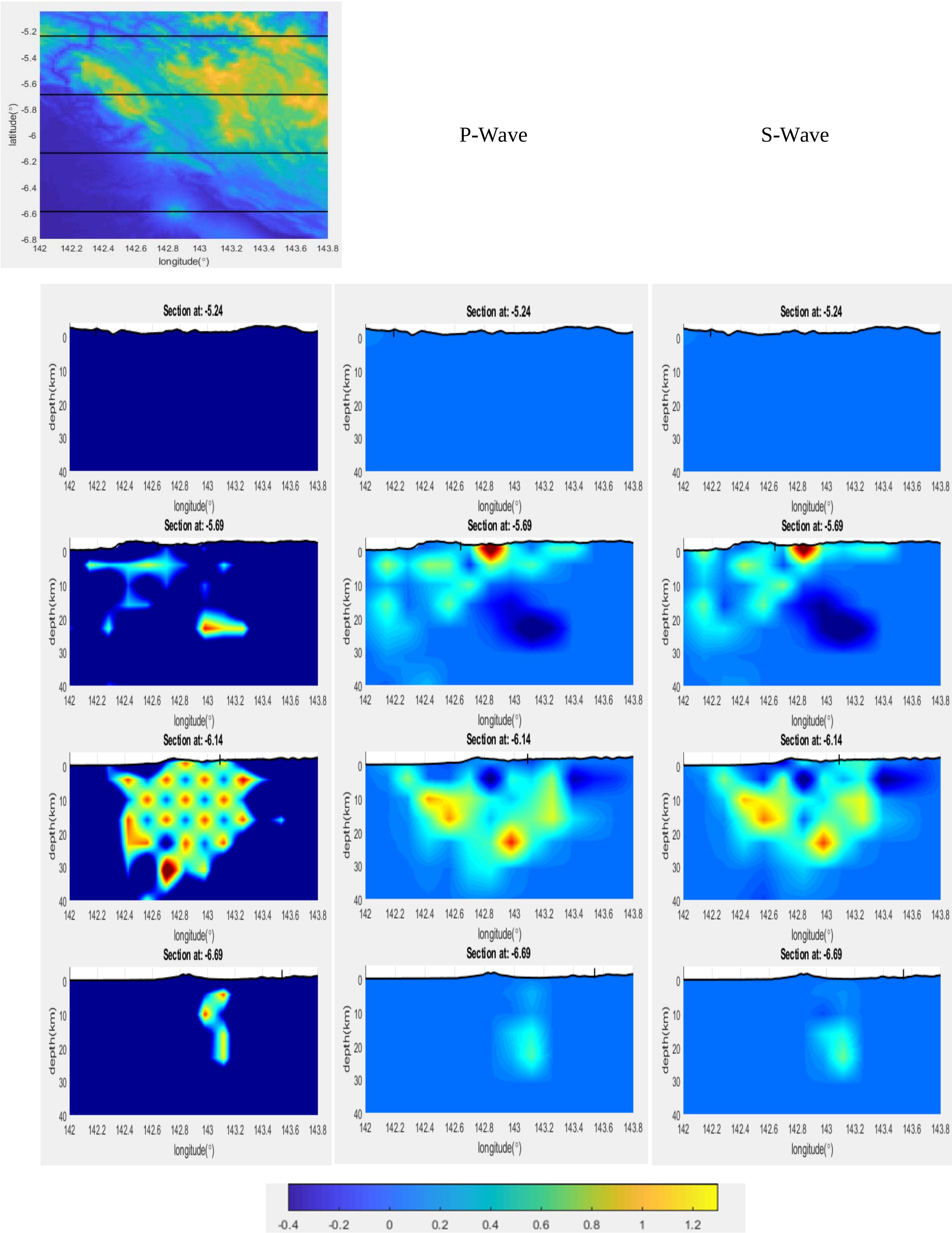

Figure 12: Checkerboard tests and latitudinal slices of relative slowness perturbation in respect to the initial velocity model; (Blue-fast, Red-Slow)

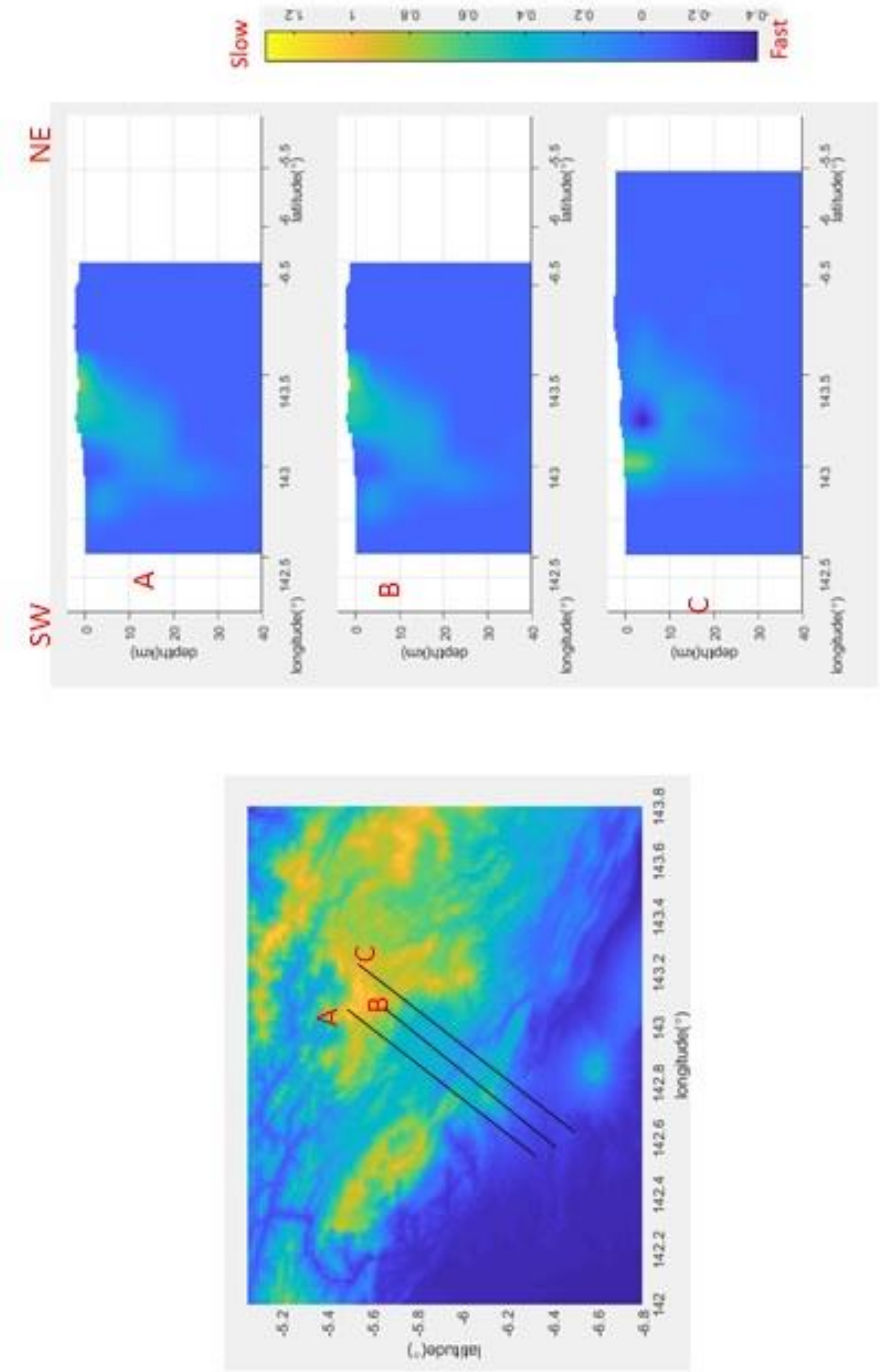

Figure 13: SW-NE cross-sections of relative slowness perturbation in respect to the initial velocity model; (Blue-fast, Red-Slow)

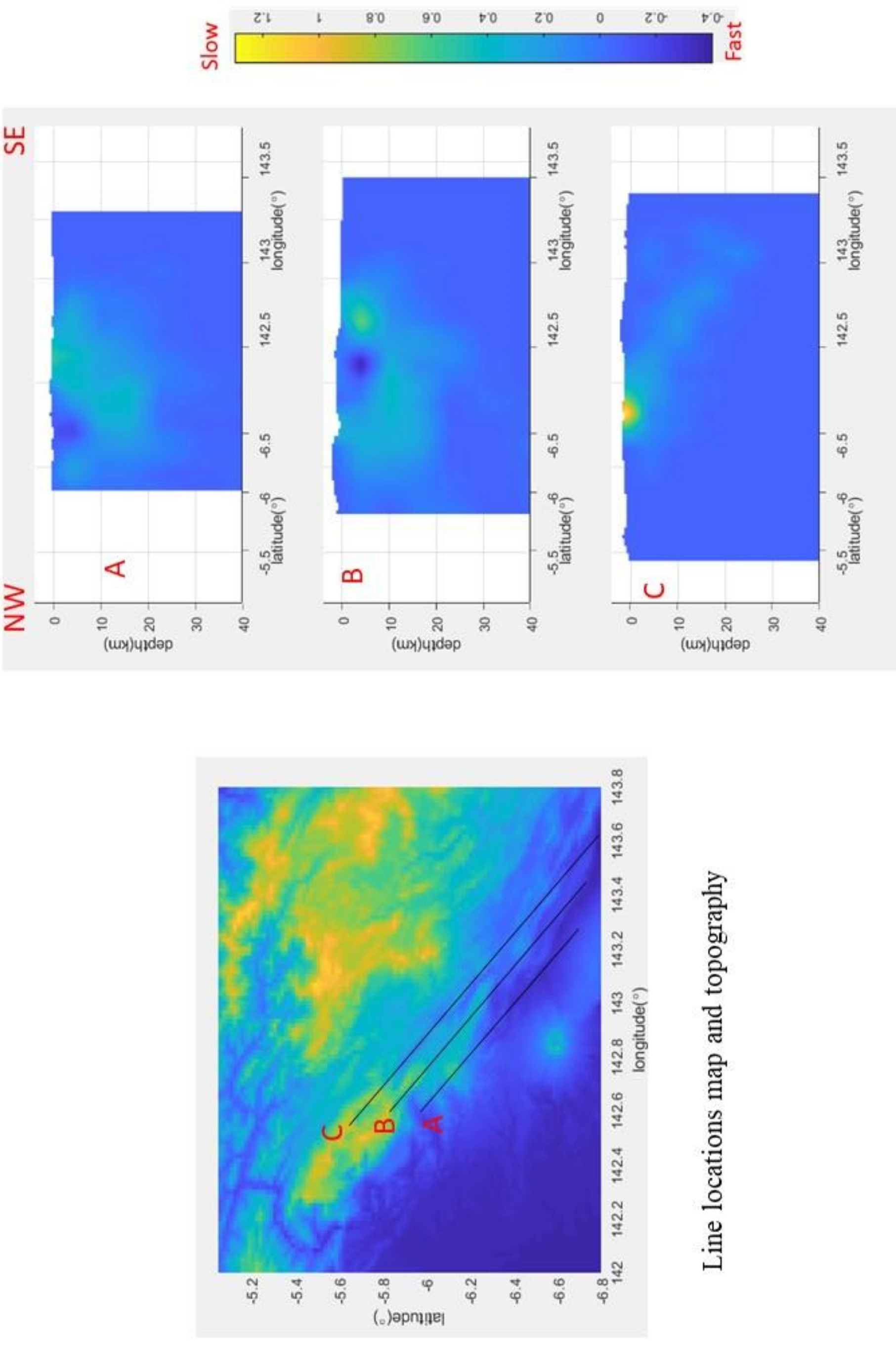

Figure 14: NW-SE cross-sections of relative slowness perturbation in respect to the initial velocity model; (Blue-fast, Red-Slow)

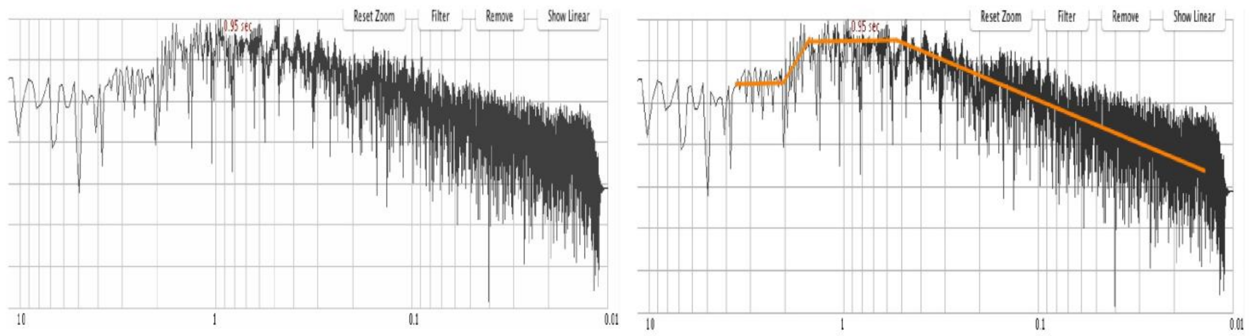

Figure 15: Fourier Spectra of the Tari Hospital ground acceleration time history, site PH01, the horizontal scale is period (sec), vertical is amplitude. Trend lines are added on the rhs figure

The tomographic study of the aftershocks is very much a work in-progress and the authors will report in more details when new results become available. 3-D variations to the velocity model have been explored with a view to revising larger number of aftershock and their locations. Although at the edge of the Australian Moho map constructed from the full set of available seismological estimates, our geotomography images are in agreement with other authors for areas underneath the Southern Highlands of PNG, where its estimated depth from the surface is approximately 40km.

McCue at al., 2018 pointed out that the records of the many examined aftershocks look alike, and are quite different from Australian earthquakes at the same distance. For one thing the dominant seismic wave frequency is lower in the Southern Highlands than at a typical Australian cratonic site, for another the first motions are invariably small and lastly some of the surface waves recorded in PNG are many times larger than the body waves. We know from a study of isoseismal maps of past earthquakes and a study of the quality factor Q in SE Australia that the ground motion attenuation is much higher in PNG, the felt area being much smaller than for a similar sized earthquake in Australia. For example, the felt area of the magnitude 7.5 mainshock on 26 February is similar to the felt area of the Newcastle NSW earthquake of 28 December 1989, its magnitude being just 5.5. This is an important factor in assessing relative or absolute earthquake hazard and risk.

Both McCue et al., 2018 and Gibson et al., 2018 emphasise that focal depth is an important parameter for modeling structural response either with a time-history analysis or a design spectra, so appropriate strong motion records are essential. Focal depth is the parameter with the highest uncertainty in locations using whole Earth models used by international seismological agencies USGS or ISC.

REFERENCES

Gibson G., McCue K. and Love, D., (2018). Analysis of Aftershocks in the Southern Highlands, Papua New Guinea. Australian Earthquake Engineering Society 2018 Conference, Nov 16-18, Perth, W.A.

McCue K., Gibson G. and Love, D., (2018). Monitoring Aftershocks in the Southern Highlands Papua New Guinea. Australian Earthquake Engineering Society 2018 Conference, Nov 16-18, Perth, W.A.

Ripper, I. D., and McCue, K. F., 1983. The seismic zone of the Papuan Fold Belt. BMR Journal of Australian Geology and Geophysics, 8, 147-156.

Salmon, M., Kennett B.L.N., Stern, T., and Aitken, A.R.A. (2012). The Moho in Australia and New Zealand, Tectonophysics-125543. Journal homepage www.elsevier.com/locate/tecto.

Sinadinovski, C., Abdulah, A., McCue, K.F., Gibson G. and Love, D. (2018). Probing the crust under the Southern Highlands of Papua New Guinea. Australian Earthquake Engineering Society 2018 Conference, Nov 16-18, Perth, W.A.

St John, V. P. (1967). The gravity field in New Guinea. Ph.D. Thesis, University of Tasmania (unpublished).